

Improving Sensitivity in Ultrasound Molecular Imaging Using a Coherence-Based Beamformer

Dongwoon Hyun^{1,2}, Lotfi Abou-Elkacem³, Juergen K. Willmann³, and Jeremy J. Dahl³

Department of Biomedical Engineering¹, Duke University

Departments of Bioengineering² and Radiology³, Stanford University



CANARY CENTER
AT STANFORD

Introduction

Molecular contrast-enhanced ultrasound (CEUS) is an imaging technique that uses targeted microbubbles (MBs) to detect a variety of molecular markers. In recent years, MBs have been used successfully for non-invasive imaging of tumor angiogenesis in pre-clinical imaging applications. However, translation to imaging in humans is challenging. Previous studies indicate that only small quantities of MBs are retained at their target sites. Clinical imaging frequencies are lower, and therefore have worse resolution. Furthermore, the intervening tissue layers between the transducer and the tumor cause image degradation via mechanisms such as **attenuation, phase aberration, and reverberation clutter**.

We propose the use of an alternative beamforming technique called **Short-Lag Spatial Coherence (SLSC)**¹. SLSC has been shown to mitigate the effects of clutter and enhance image quality in noisy conditions *in vivo*, and can be used to enhance low-amplitude coherent echoes from targeted MBs.

Spatial Coherence of Backscatter

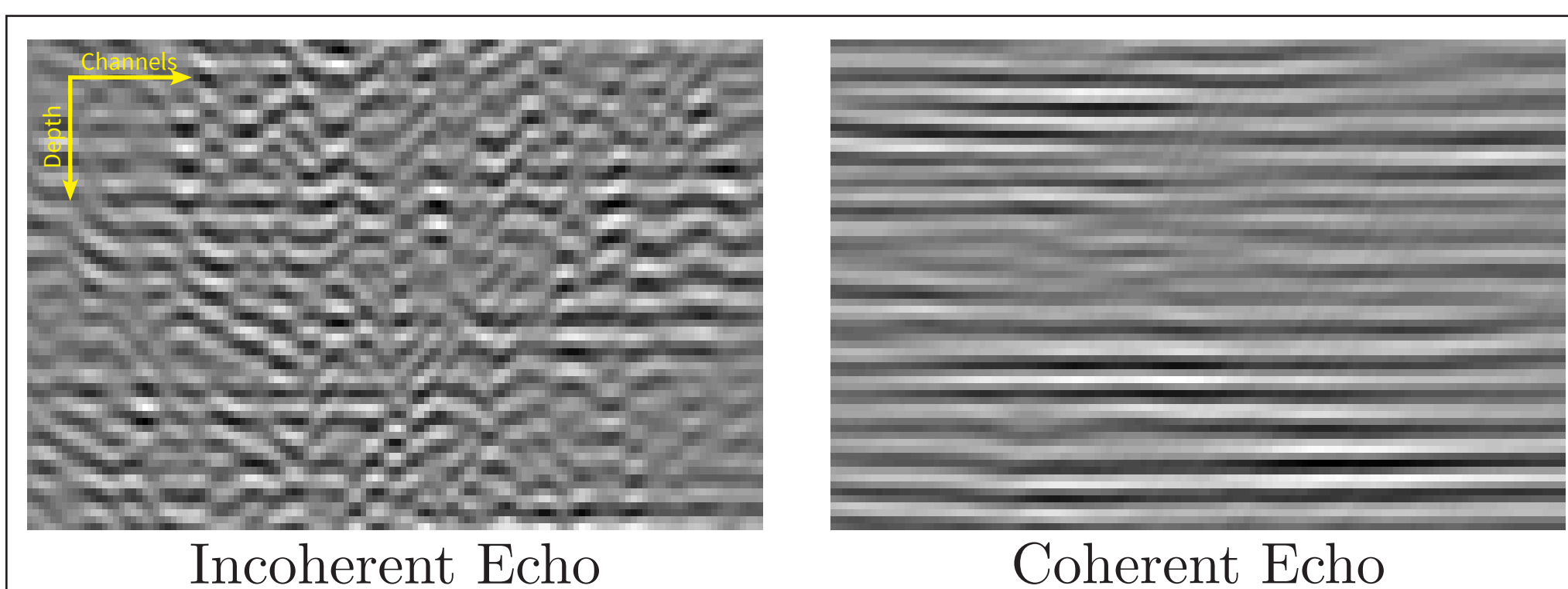


Figure 1. Spatially incoherent and coherent echoes are shown above. SLSC images show the level of coherence in an echo rather than its magnitude.

The spatial coherence of an echo is a measure of its similarity at different channels across the transducer surface. It is measured as the average correlation coefficient at a channel spacing of m :

$$\hat{R}(m) = \frac{1}{N-m} \sum_{i=1}^{N-m} \frac{s_i s_{i+m}^*}{|s_i| |s_{i+m}|}$$

where N is the number of channels, s_i is the echo received by the i -th channel, and $*$ denotes the complex conjugate. The coherence of backscatter is dependent upon its source (Fig. 2), and can be used to enhance MB signals and help suppress signals from tissue and incoherent noise.

An SLSC image pixel is computed by integrating the spatial coherence function over small lags up to some threshold M :

$$V_{\text{SLSC}} = \int_1^M \hat{R}(m) dm$$

M is often selected to be a quarter of the aperture ($N/4$).

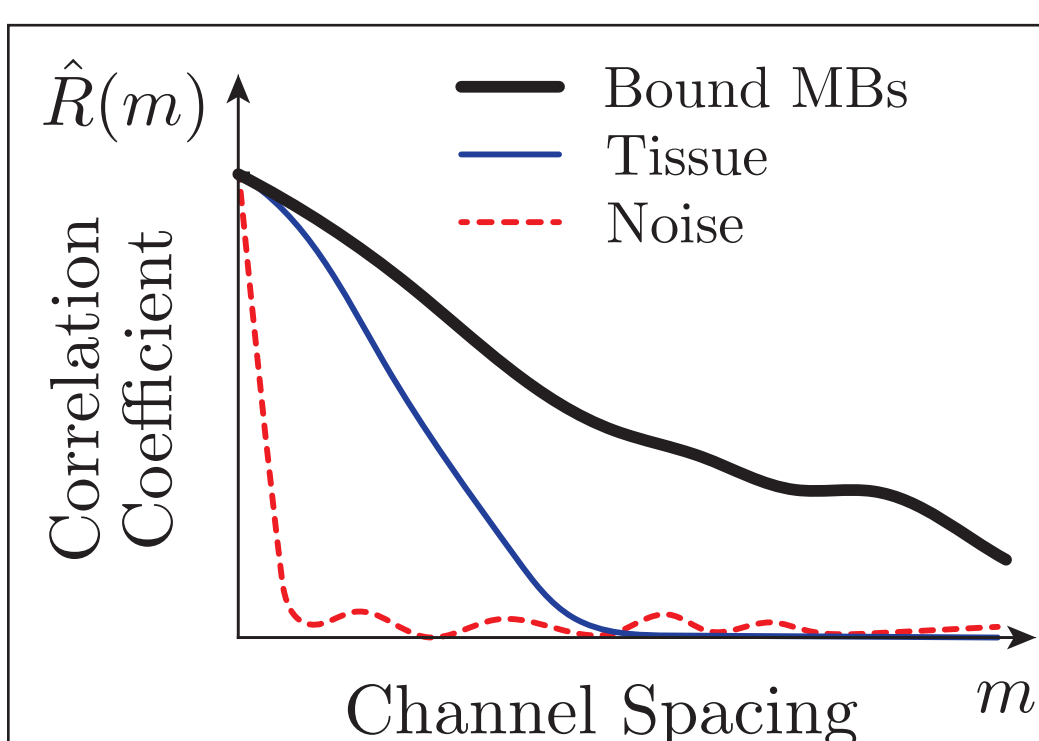


Figure 2. In SLSC, the correlation coefficients are computed as a function of channel spacing. Point scatterers (e.g., bound MBs), diffuse scatterers (e.g., tissue), and noise (e.g., reverberation clutter) have distinct correlation profiles that are most distinguishable at small values of m , referred to as "short lags".

Materials and Methods

A research ultrasound scanner was used to acquire 128 channels of RF from a linear array transducer receiving at 10 MHz. A plane wave synthetic aperture technique was combined with pulse-inversion harmonic imaging, and the received channel data were processed with a GPU-based software beamformer, displaying both conventional and the proposed SLSC-CEUS images side-by-side in real time.

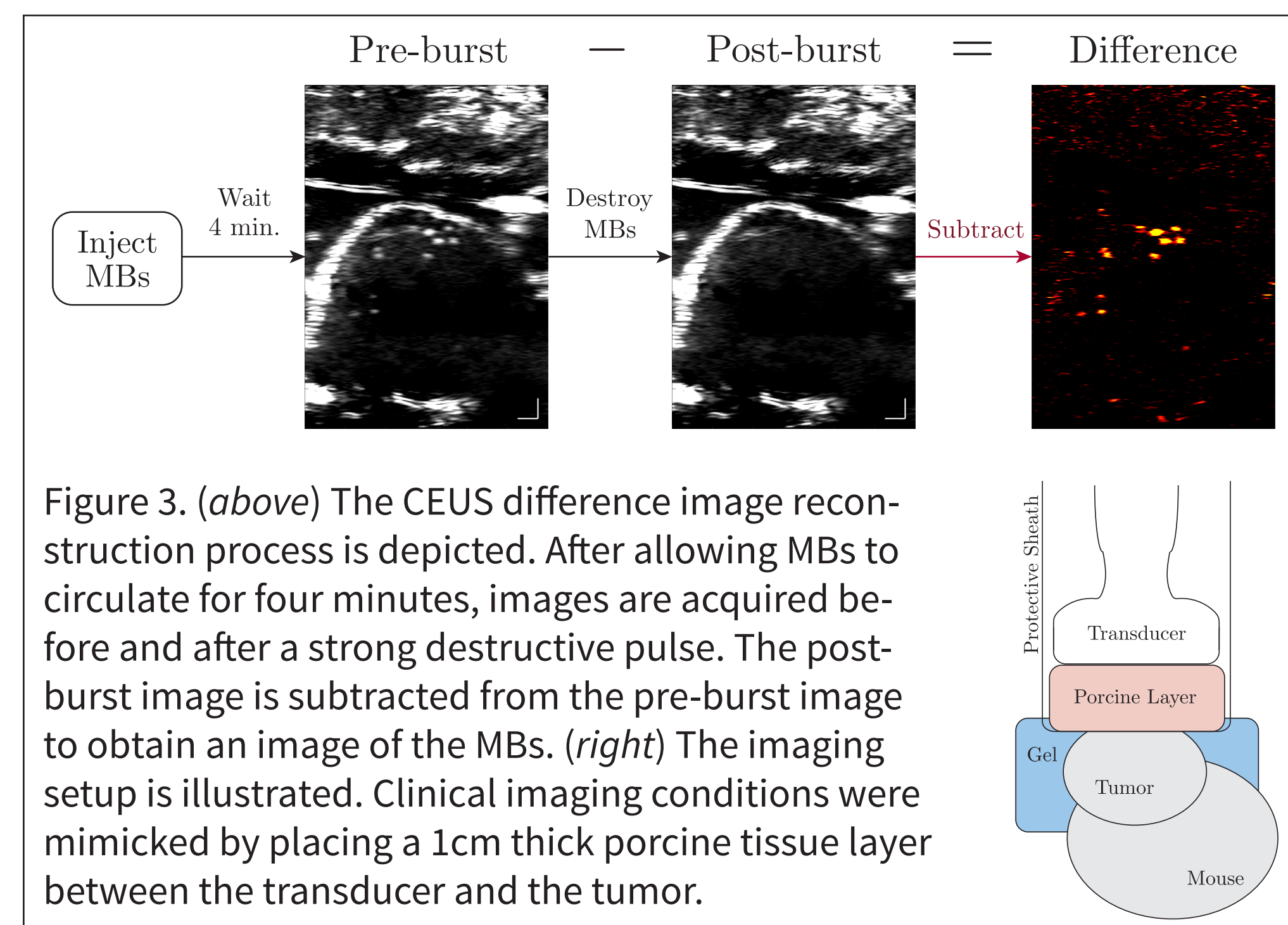


Figure 3. (above) The CEUS difference image reconstruction process is depicted. After allowing MBs to circulate for four minutes, images are acquired before and after a strong destructive pulse. The post-burst image is subtracted from the pre-burst image to obtain an image of the MBs. (right) The imaging setup is illustrated. Clinical imaging conditions were mimicked by placing a 1cm thick porcine tissue layer between the transducer and the tumor.

In vivo experiments were performed in a mouse model of hepatocellular carcinoma, with a xenografted subcutaneous tumor on the hind limb of the animal. 10 tumors were imaged in total. Clinical grade MBs were targeted to VEGFR2. A solution containing a concentration of 5×10^7 MB/mL was injected into a blood vessel in the tail, and difference images were formed via the process illustrated in Fig. 3. The sensitivity to the MB signal was measured using the SNR, defined as the ratio of the RMS MB signal to the RMS porcine tissue signal:

$$\text{SNR} = 20 \log_{10} \frac{\text{RMS} [I_{\text{diff}}(\text{Microbubbles})]}{\text{RMS} [I_{\text{diff}}(\text{Tissue})]}$$

Results

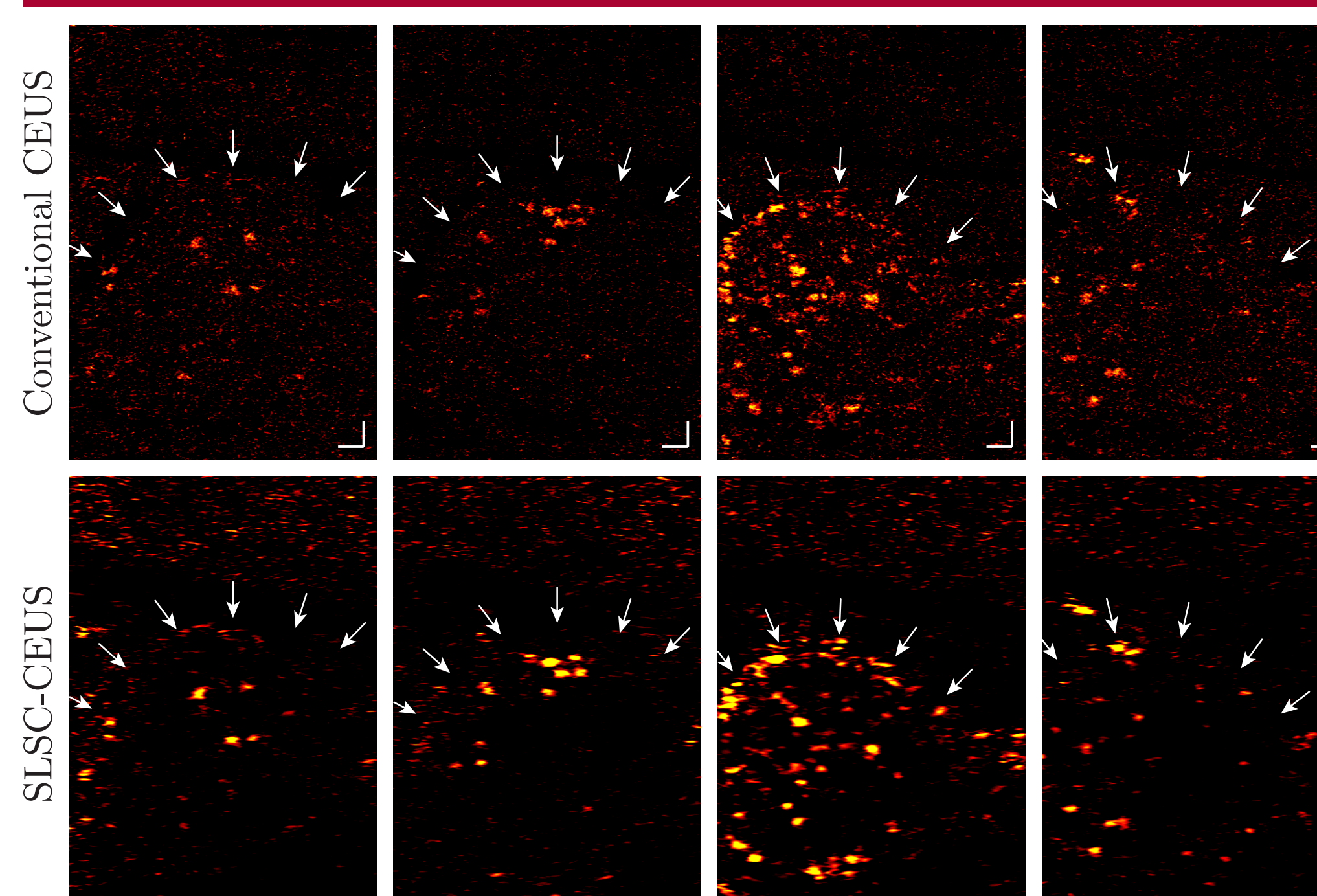


Figure 4. Examples of low MB retention in a mouse tumor. CEUS difference images were formed using the conventional (top row) and SLSC (bottom row) techniques. The white bars show 1mm, and the arrows show the outline of the tumor. The images display a dynamic range of 1 to 5 times the RMS of the noise floor, as measured in the porcine tissue layer above the tumor. SLSC-CEUS enhances the MB signal while reducing noise in the surrounding tissue.

Results (continued)

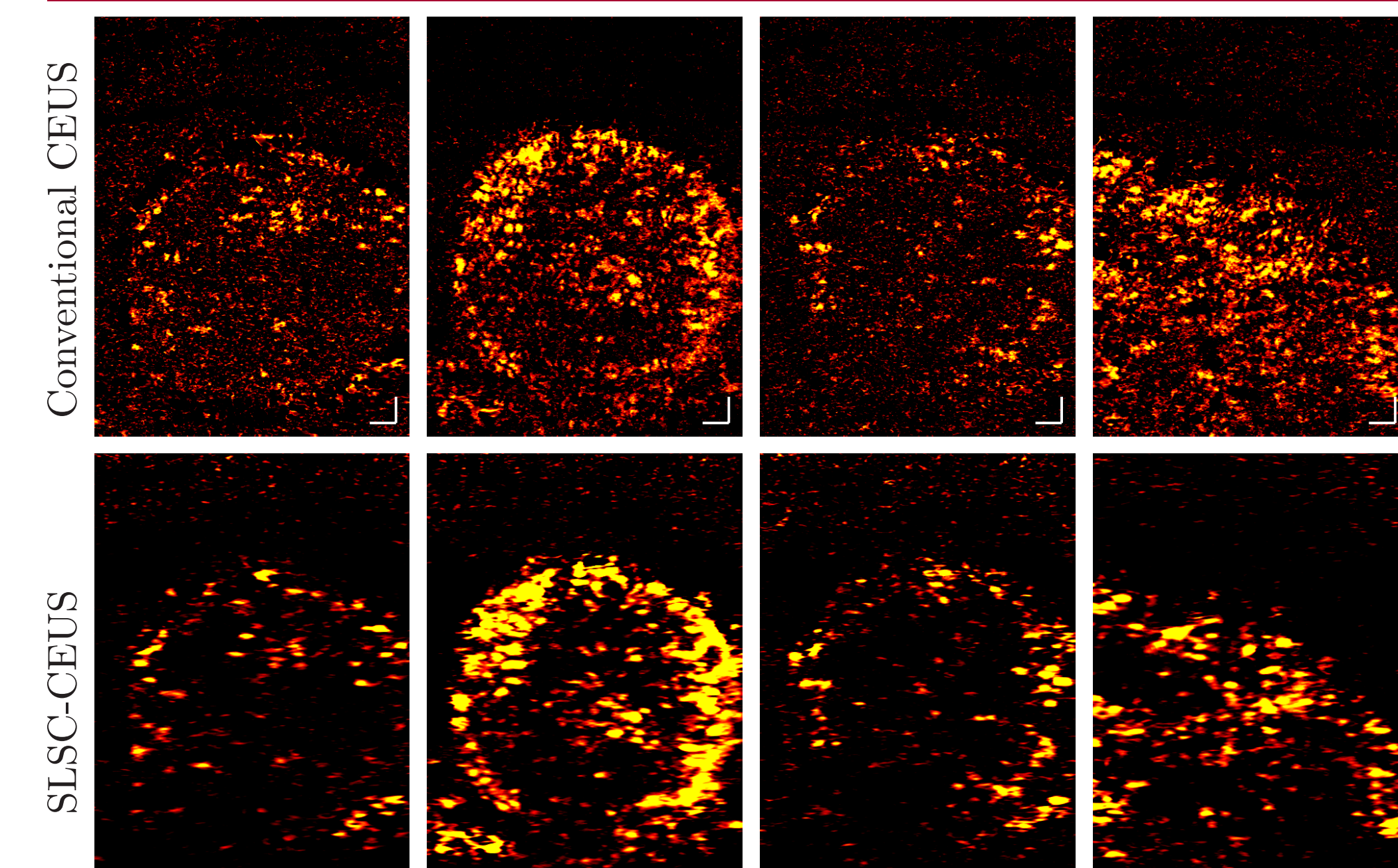
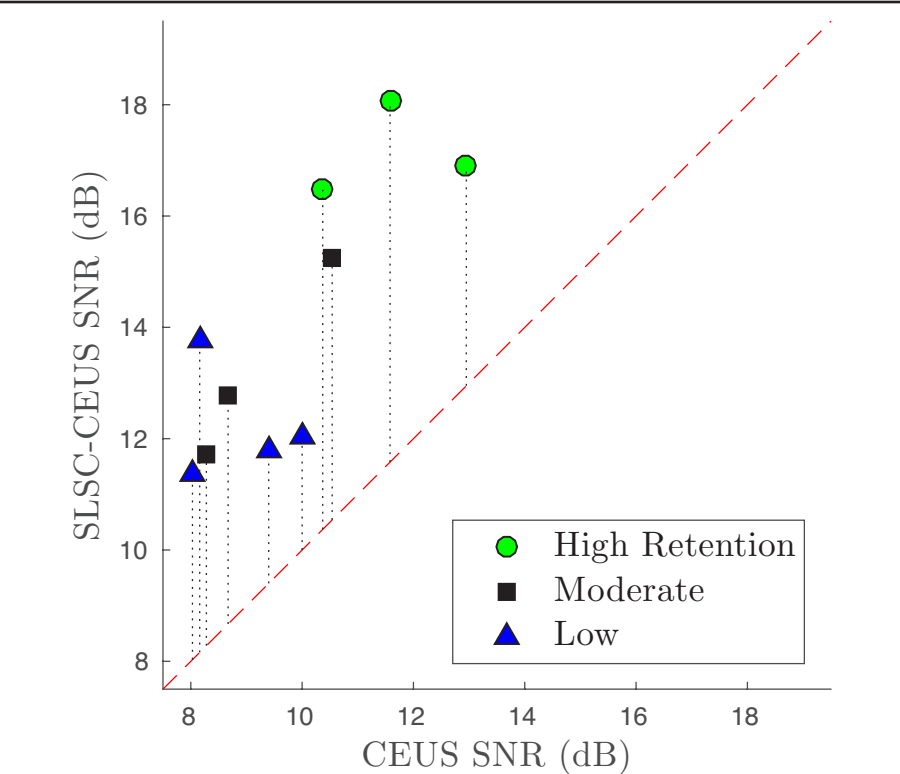


Figure 5. Examples of moderate to high MB retention. Conventional (top) and SLSC (bottom) CEUS difference images are shown. The images display a dynamic range of 1 to 5 times the RMS of the noise floor. Individually bound MBs are the background with SLSC-CEUS.

Figure 6. The sensitivities of the SLSC-CEUS images are plotted against those of the conventional CEUS images. In the presence of the porcine layer, SLSC-CEUS improved the SNR in each of 10 separate acquisitions with varying levels of MB retention in the tumor. The average improvement in SNR was 65%, corresponding to 4.3dB SNR.



Discussion

In this study, *in vivo* imaging conditions were mimicked using a layer of porcine tissue. SLSC-CEUS improved the sensitivity in every acquisition, with an average increase of 65% in SNR. The clutter and noise generated *in vivo* is often spatially incoherent but high in magnitude. The conventional CEUS beamformer, which detects magnitude, interprets the noise as signal. The SLSC beamformer instead detects regions that scatter off echoes with high spatial coherence, regardless of magnitude. This allows SLSC-CEUS to identify echo sources that are weak in magnitude but high in spatial coherence, such as individually bound MBs, and to suppress noise that is high in magnitude and spatially incoherent.

Conclusions

The SLSC beamformer improves sensitivity to targeted MBs in conditions similar to clinical imaging by utilizing the spatial coherence of the echo, and may pave the way for the early detection of cancer in humans.

Acknowledgments

This work was supported by NIH grants R01-EB013661 and R21-EB022770 from the NIBIB and from a grant by the Canary Center at Stanford for Early Cancer Detection.

References

[1] Lediju, M. A., Trahey, G. E., Byram, B. C., & Dahl, J. J. (2011). Short-lag spatial coherence of backscattered echoes: imaging characteristics. *IEEE Trans. Ultrason., Ferroelect., Freq. Control*, 58(7), 1377–88.